Proceedings of the Korean Nuclear Society Autumn Meeting
Taegu, Korea, October 1997

Hydraulic Characteristics of HANARO Fuel Bundles

S. Cho, H. J. Chung, S. Y. Chun, S. K. Yang, and M. K. Chung

Korea Atomic Energy Research Institute,
P.O. Box 105, Yusong, Taejon, 305-600, Korea
Fax : +82-42-868-8362

ABSTRACT

This paper presents the hydraulic characteristics measured by using LDV(Laser Doppler Velocimetry) in subchannels of a HANARO, KAERI research reactor, fuel bundle. The fuel bundle consists of 18 axially finned rods with 3 spacer grids, which are arranged in cylindrical configuration. The effects of the spacer grids on the turbulent flow were investigated by the experimental results. Pressure drops for each component of the fuel bundle were measured, and the friction factors of fuel bundle and loss coefficients for the spacer grids were estimated from the measured pressure drops. Implications regarding the turbulent thermal mixing were discussed. Vibration test results measured by using laser vibrometer were presented.

I. INTRODUCTION

A research reactor with $30\,MW_{th}$, HANARO, is being operated in the KAERI. The HANARO fuel bundle consists of 18 fuel elements which have eight axial rectangular fins on the outer cladding to enhance the heat transfer performance. Thus the fuel bundle is characterized by the presence of a number of axial fins on the cladding. But comparing with LWR and FBR fuel bundles, the study on the fuel bundles with axially finned rods is relatively scarce. Yang et al.[1] performed the turbulent measurement in an axially finned rod bundle without spacer grids. They observed turbulent flow characteristics in the developing and developed flow area.

In this study, the detailed hydraulic characteristic measurements were preformed in subchannels of an axially finned rod bundles with spacer grids by using LDV. Axial velocity and turbulent intensity were measured. Implications regarding the turbulent thermal mixing due to spacer grids were discussed. Pressure drops for each component of the rod bundle were also measured to estimate the friction factors in rod bundles and loss coefficients for the spacer grids.

II. EXPERIMENTAL METHOD

A. Test Fuel Bundle and Test Loop

A schematic diagram of the test loop is shown in Fig. 1. The test loop consists of a variable-speed motor pump, a storage tank, a test section, and related piping. Axial configuration of the test section with a test fuel bundle is shown in Fig. 2 including the components of the fuel bundle and pressure tap locations. The circular housing of the test section is made of an acrylic tube to provide access for laser beams to the location where the velocity measurement is to be preformed. Working fluid, water, flows upward through the test section and the flow rate is measured by a turbine flow meter. A pressure transmitter and 8 differential pressure transmitters are used to measure pressure and pressure drop respectively. Vibration amplitude of each fuel bundle is measured by using laser vibrometer. The cross sectional view of the test section is illustrated in Fig. 3, which shows main dimensions and major

turbulent phenomena in subchannels. The rods were arranged in a triangular and a square array with P/D =1.52, W/D =1.32. During the experiment the water temperature was Controlled by a temperature control unit at 40 °C.

III. RESULTS AND DISCUSSIONS

A. Pressure Drops

The pressure drops for each component of a fuel bundle were measured under various flow rate conditions. The pressure drop due to the spacer grid (ΔP_G) is related to the bulk average fluid velocity, U_{av}, in the rod bundle.

$$\Delta P_G = C_B \rho \frac{U_{av}^2}{2}. \quad (1)$$

Figure 4 shows the loss coefficients of the spacer grid and a fitted correlation of them. Nearly same results were shown with that of the tube spacers axially connected in Ref. 2. In Fig. 5, the friction factors in rod bundles were estimated from the measured pressure drops, and compared with Moody's correlation for smooth tubes. The friction factors were calculated as

$$f = -\frac{dP}{dx}\frac{D_h}{2\rho U_{av}^2}. \quad (2)$$

The result shows that the friction factors for axially finned rod bundles are less than the values given by Moody's curve, which coincides with the results of Grover and Venkat Raj[3] study on the flow in seven rod bundles with three axial fins, P/D = 1.224, and W/D = 1.047.

B. Axial velocity

Turbulent velocity measurements were performed at axial locations L/D_h = 2, 7, 14, and 23 in each grid span, and transversing Paths A and B (Fig. 3). Axial measuring length L is calculated from upper surface of each grid. Figure 6 shows the developing axial velocity profiles in each grid span at Path A. The velocities are not fully developed in every grid span. The velocity profiles in the first grid span are different from those of the other spans. However, from the second span, the velocity profiles develop in the same manner each other. This is due to the difference of the shape between bottom end plate and spcer grids.

C. Axial Turbulent Intensity

Figure 7 represents the axial turbulent intensity in the first and third grid span at Path A with varing the axial locations. The higher intensities are distributed at $L/D_h = 2$ near the lower spacer grid. The intensities decrease to the lowest values at $L/D_h = 23$. Axial turbulent intensities at Points 1-4 (Fig. 8) as function of axial locations are shown in Fig. 9. The highest intensities are observed immediately downstream of the bottom end plate and each spacer grid, and they decay rapidly to the stable values.

In Figs. 10, the turbulence decay for each grid span was compared with the correlation reported by Yang and Chung[4], that is,

$$\frac{\overline{u^2}}{U^2} = 0.04\ (x/P)^{-1.2}. \quad (3)$$

This is obtained from the PWR mixing spacer grids. Similar trends were observed.

D. Implications Regarding Turbulent Thermal Mixing

In a possible way to analyze thermal hydraulic behavior of the fluid at the spacer grid, the relation between heat and momentum transfer in turbulent flow can give information on the thermal behavior near spacer grid. If the enthalpies and velocities of the neighboring subchannels are different, an exchange of energy and momentum flux will occur. The expressions for the net turbulent energy flux, F_h, and momentum flux, F_m, between subchannels can be given, respectively, by Stewart, et al[5].

$$F_h = \rho\, w_{eff}\, \Delta h, \tag{4}$$

$$F_m = F_t\, \rho\, w_{eff}\, \Delta U\ . \tag{5}$$

The turbulent cross-flow flux can be expressed as diffusive energy flux between centroids of subchannels, by introducing a mixing factor [6-7], can be given as

$$F_h = \varepsilon\, Y \rho\, \Delta h / \Delta y \tag{6}$$

, where the eddy viscosity at the center of a circular tube, i. e.,

$$\varepsilon = \nu\, (f_{Dt}/8)^{0.5}\ Re/20\ [8] \tag{7}$$

Equating Eq. (4) to Eq. (6) yields

$$Y = w_{eff}\ \Delta y/\varepsilon. \tag{8}$$

Since w_{eff} is not available in the present measurement, $w_{eff} \fallingdotseq u'$ was assumed at the central region in the gap[6]. Local mixing factor nondimensionalized by Y_0, which is the local value in the fully developed flow region without spacer grid, is shown in Fig. 11. Y_0 was assumed from the results of Yang et al.[1]. As shown in Fig. 11, turbulent mixing occurs actively in immediate downstream region of each spacer grid, and beyond this region the mixing occurs steadily.

E. Vibration Amplitude

Peak, RMS amplitude and frequency characteristics are obtained from the signal of vibrometer by FFT analysis. Vibration levels are measured at two points(view port1,2, 90° rotated position) of a grapple head of each HANARO fuel bundle. Figure 12 shows RMS amplitude of a 18-element fuel bundle as a function of flow rate. At view port 1, the values which are measured after endurance test are some higher than those of which measured before endurance test. At view port 2, the RMS values show nearly same trend and level.

F. Uncertainty Analysis

Experimental uncertainties in the measured quantities were evaluated according to the ANSI/ASME PTC 19.1 Code[9]. Accuracy of each instrument was used as a Bias error and the Precision error was evaluated from the standard deviation of the each measured parameter. Uncertainties of loss coefficient and friction factor are 2.8 and 3.4%, respectively. And the uncertainties of average velocity(U), turbulent intensity, and mixing factor are 2.9, 11, and 8.5%, respectively.

IV. CONCLUDING REMARKS

This study measured the detailed hydraulic characteristics in subchannels of axially finned rod bundle with spacer grids. The experimental results led to the following conclusions:

(1) The friction factors for the axially finned rod bundle in this study are less than those given by Moody's correlation for smooth tubes.

(2) The velocity profiles are not fully developed in the full flow channel. The velocity profiles in the downstream span of the bottom end plate are different from those of the other spans.

(3) The axial turbulent intensity is highest immediately downstream of each grids, and decays to a stable level as the flow develops.

(4) The turbulent mixing occurs actively in immediate downstream region of each spacer grid, and beyond this region the mixing occurs steadily.

NOMENCLATURE

f_{Dt}	friction factor of a circular tube
u	axial fluctuating velocity , m/s
u'	rms value of u, m/s
W	wall distance, m
W_{eff}	effective mean mixing velocity

Y mixing factor

Δy centroid or mixing distance between subchannels, m

Greek symbols

ε turbulent eddy viscosity, m^2/s

ν kinematic viscosity, m^2/s

REFERENCES

[1] S. K. Yang, M. K. Chung and H. J. Chung, "Measurements of Turbulent Flow in Axially Finned Rod Bundles," Experimental Thermal and Fluid Science, 5, 828-837 (1992)

[2] K.Rehme, "Pressure Drop Correlations for Fuel Element Spacers", Nuclear Technology, 17, 12-23 (1973)

[3] R. B. Grover, and V. Venkat Raj, "Pressure Drop Along Longitudinally Finned Seven-Rod Cluster Nuclear Fuel Elements," Nucl. Engrg. Des. 58, 79-83 (1980)

[4] S. K. Yang, and M. K. Chung, "Turbulent Flow through Mixing Spacer Grids in Rod Bundles", National Heat Transfer Conference, 14, 33-40 (1995)

[5] C. W. Stewart et al.,"COBRA-IV:the Model and the Method", Battele, Pacific Northwest Laboratories (1977)

[6] S. V. Möller, "Single-phase Turbulent Mixing in Rod Bundles", Experimental Thermal and Fluid Science, 5, 26-33 (1992)

[7] K. Rehme, "The Structyre of Turbulence in Rod Bundles and the Implications on Natural Mixing between the Subchannels", Int. J. Heat Mass Transfer, 35, 567-581 (1992)

[8] L. Ingesson and S. Hedberg, "Heat Transfer between Subchannels in a Rod Bundles", Heat Transfer, Vol. III, Fc.7.11 (1970)

[9] ANSI/ASME PTC 19.1, "ASME Performance Test Codes : Supplement on Instruments and Apparatus, Part-1 ; Measurement Uncertainty" (1985)

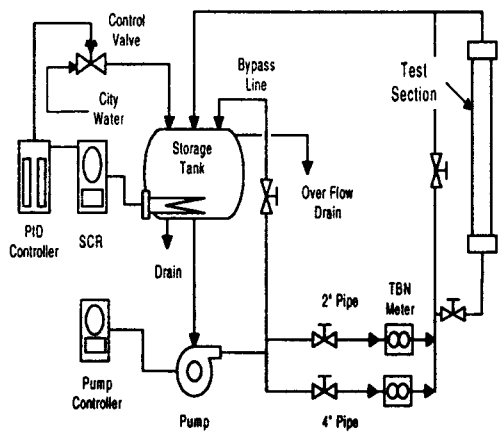

Fig. 1 Schematic Diagram of the Test Loop

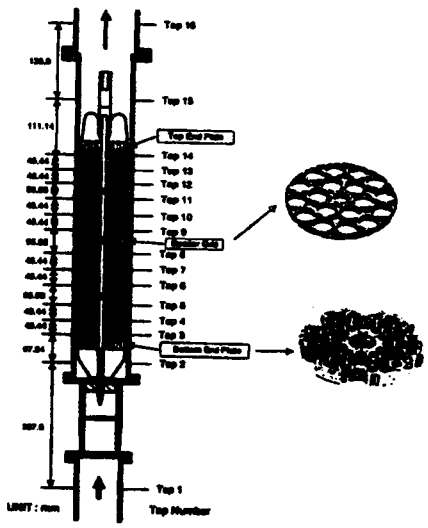

Fig. 2 Axial Configuration of Rod Bundle with Spacer Grids

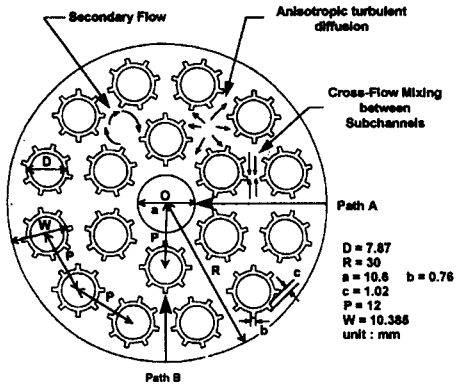

Fig. 3 Turbulent Phenomena in Subchannels

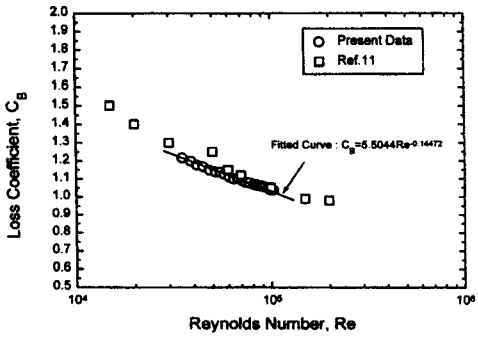

Fig. 4 Loss Coefficient of the Spacer Grid

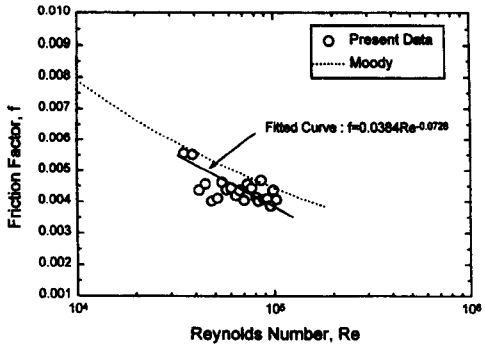

Fig. 5 Friction Factor for the Rod Bundle with Spacer Grid

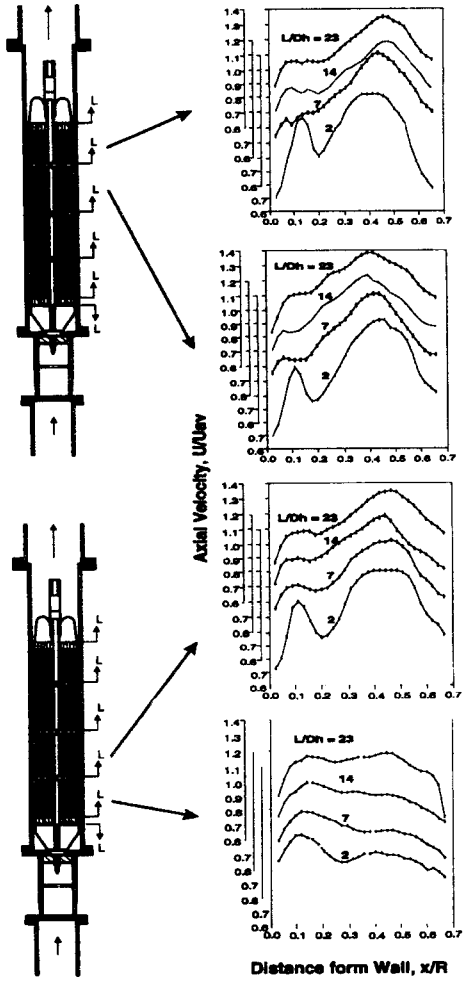

Fig. 6 Developing Axial Velocity at Path A

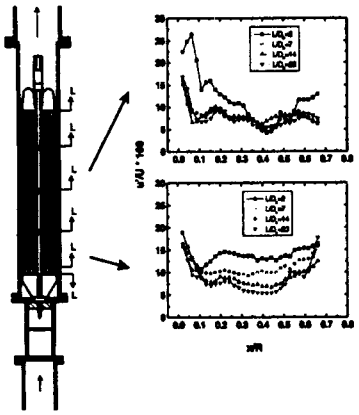

Fig. 7 Axial Turbulent Intensity at Path A

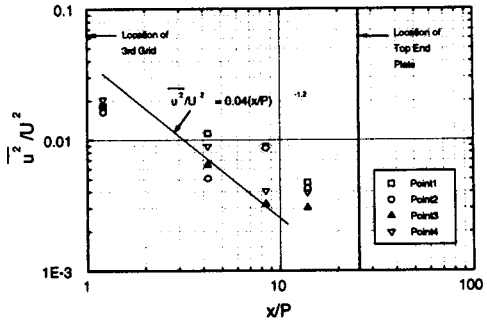

Fig. 10 Axial Turbulent Intensity Decay Downstream of 3rd Spacer Grid

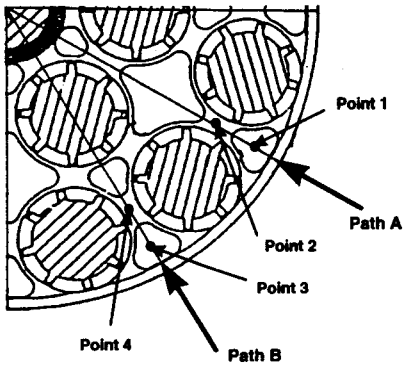

Fig. 8 Measuring Points of Turbulent Decay

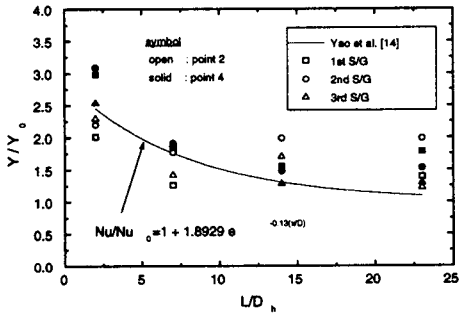

Fig. 11 Local Mixing Factor Downstream of Each Spacer Grid

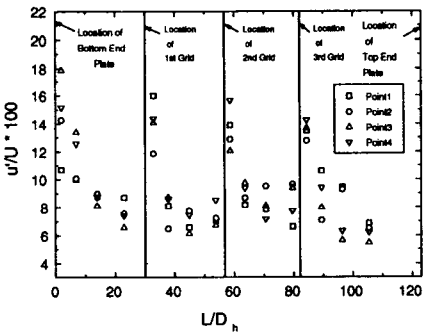

Fig. 9 Axial Turbulent Intensity Decay

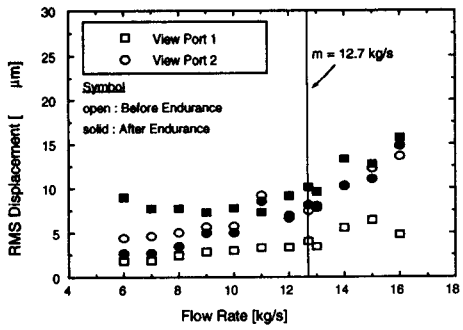

Fig. 12 RMS Displacement as a Function of Flow Rate